IEEE Photonics Journal
An IEEE Photonics Society Publication

Open Access

Firelight LED Source: Toward a Balanced Approach to the Performance of Solid-State Lighting for Outdoor Environments

Volume 6, Number 3, June 2014

A. Žukauskas, Senior Member, IEEE
R. Vaicekauskas
A. Tuzikas
A. Petrulis
R. Stanikūnas
A. Švegžda
P. Eidikas
P. Vitta

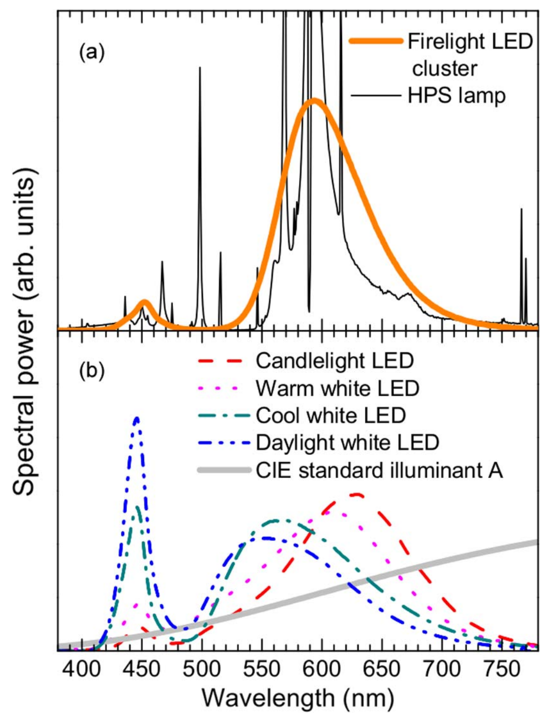

DOI: 10.1109/JPHOT.2014.2319102

Firelight LED Source: Toward a Balanced Approach to the Performance of Solid-State Lighting for Outdoor Environments

A. Žukauskas,[1] *Senior Member, IEEE*, R. Vaicekauskas,[2] A. Tuzikas,[1] A. Petrulis,[1] R. Stanikūnas,[3] A. Švegžda,[3] P. Eidikas,[1] and P. Vitta[2]

[1]Institute of Applied Research, Vilnius University, 10222 Vilnius, Lithuania
[2]Department of Computer Science, Vilnius University, 08303 Vilnius, Lithuania
[3]Department of General Psychology, Vilnius University, 01513 Vilnius, Lithuania

DOI: 10.1109/JPHOT.2014.2319102

Manuscript received March 13, 2014; revised April 9, 2014; accepted April 12, 2014. Date of publication April 23, 2014; date of current version May 2, 2014. This work was supported by the Lithuanian Research Council under Grant ATE01/2012. The work of P. Vitta was supported by the European Union Structural Funds through the Project "Postdoctoral Fellowship Implementation in Lithuania."
Corresponding author: A. Tuzikas (e-mail: arunas.tuzikas@tmi.vu.lt).

Abstract: We report on a blue-amber ("firelight") cluster of light-emitting diodes (LEDs) with extra-low correlated color temperature (~1860 K) optimized for outdoor lighting under mesopic conditions. When compared with common white LEDs, the firelight LED cluster shows considerably reduced indexes of melatonin suppression and skyglow, increased retinal illuminance for elderly people, but a reduced performance of perceiving colors, which, however, can be tolerated at mesopic luminance. In comparison with an almost metameric high-pressure sodium lamp, the cluster exhibits a potentially higher luminous efficacy, similar reaction time and detection threshold of luminance contrasts for achromatic targets, and noticeably improved color discrimination characteristics.

Index Terms: Light emitting diodes, solid-state lighting, outdoor lighting, photophysiology, light pollution, psychophysics, color rendition, color discrimination.

1. Introduction

The energy efficiency and reliability offered by solid state-lighting technology brought to a massive replacement of high-pressure sodium (HPS) lamps by light-emitting diodes (LEDs) in outdoor illumination. LEDs are efficacious, longevous, have improved directionality, and are easy to intelligently control [1]–[3]. In addition, the needs in color rendition and color discrimination can be better met, since the spectral power distribution (SPD) of LED-based sources can be versatilely tailored through the conversion of short-wavelength electroluminescence in semiconductor chips to photoluminescence in different phosphors or through assembling clusters of LEDs having different colors [4], [5].

Common white phosphor converted (pc) LEDs have short-wavelength rich SPDs and their luminous efficacy increases with reducing adaptation luminance (L) due to the Purkinje effect, which is the short-wavelength shift of the spectral sensitivity of the human eye. This has been claimed as an additional advantage of LEDs for outdoor lighting in respect of common HPS lamps, which have blue-deficient SPD and reduced luminous efficacy at low luminances [2]. However, switching from blue-deficient light sources (typically, HPS lamps) to blue-enriched ones (metal-halide lamps and, presently, LEDs) in outdoor lighting created numerous concerns and issues that are being actively debated [6]. In particular, with the discovery of intrinsically photosensitive retinal ganglion cells (ipRGCs), which contain blue-light absorbing melanopsin photopigment [7]–[9], the application of blue-enriched light in night-time environments was recognized to be harmful due to the unwanted non-visual photobiological effect (suppressing pineal melatonin production and shifting melatonin phase), which disrupts circadian rhythms and poses serious health issues even at low illuminances [10]–[17]. Also, light pollution due to molecular (Rayleigh) and aerosol (Mie) scattering causes increased urban skyglow in the vicinity of blue-enriched light sources. Such skyglow has a detrimental effect on astronomical research [6], [17], [18] and ecological processes [19]. One more important issue is the aggravation of night-time driving conditions for elderly people due to the yellowing of the lenses of the eye with age [17], [20]. For equal conditions of ambient luminance, such a yellowing results in a reduction of retinal illuminance under blue-enriched light in addition to that due to the age-related decrease of the overall optical transmission of the lenses. Finally, some outdoor lighting environments can lose aesthetic attractiveness when switching from HPS lamps to common white LEDs, which have a higher CCT. This unwanted effect may occur according to the Kruithof hypothesis [21], which suggests that for illuminances typical of outdoor lighting, the lighting is considered pleasing when the light source has a CCTs below 2500 K. Although this hypothesis has been the subject of controversy for years [22], [23], recently it has been partially validated in that the of impressions of comfort, pleasantness and relaxation increase, when CCT decreases [24].

The above concerns and issues indicate on the necessity of the adaptation of solid-state lighting technology to the specific needs of outdoor lighting with a balanced approach to improving efficacy and color quality, on the one hand, and avoiding photobiological hazards, light pollution, discrimination of elderly drivers, aesthetic inconvenience, and other issues related to the use of blue-enriched light at nighttime, on the other hand.

Recently, the SPDs of LED-based sources of light have been numerically optimized for low-luminance photobiologically-friendly lighting applications [25]. The optimal SPDs have extra low CCTs and are composed of two components, a narrow-band blue one peaked in the range around 440 nm and a wider-band complementary one peaked in the yellow-orange range of the spectrum. Such dichromatic light sources, which are the solid-state counterparts of HPS lamps, have been designated in [25] as "firelight" solid-state lamps. The firelight lamps have the lowest partial power in the short-wavelength region of the visible spectrum out of all solid-state sources of light with the chromaticity close to that of the blackbody. They can be composed of either clusters of blue and amber colored LEDs or implemented as single-package LEDs with the partial conversion of blue electroluminescence to amber photoluminescence in phosphors [26]. (One more approach to the development of low-CCT LEDs is based on the reduction of short-wavelength spectral power of common white LEDs using optical filters [27]; however, such an approach lacks reasoning from the standpoint of the inherent concept of solid-state lighting technology, which is based on the straightforward tailoring of SPD without introducing optical losses.)

In this paper, we present the results of the assessment of visual and non-visual performance characteristics of a practical firelight (blue-amber) LED cluster metameric to a HPS lamp. In particular, the SPD of the firelight cluster has been assessed in the mesopic range of luminances typical of outdoor lighting by quality indices relevant to different lighting issues (efficacy, color rendition, melatonin suppression, skyglow, and eye lens yellowing) and compared to those of common white LEDs and sodium-based light sources. Also, psychophysical performance characteristics relevant to driving (time of reaction to achromatic stimulus, detection threshold of luminance contrasts for achromatic targets, and color discrimination) have been measured against the HPS counterpart in laboratory under mesopic vision conditions.

2. Firelight LED Cluster

An experimental firelight LED cluster was assembled of eight pc amber LEDs (Philips Lumileds model Luxeon Rebel LXM2-PL01) and one InGaN direct emission royal blue LED (LXML-PR02) with peak wavelengths of 594 nm and 452 nm, respectively. The peak wavelengths of the

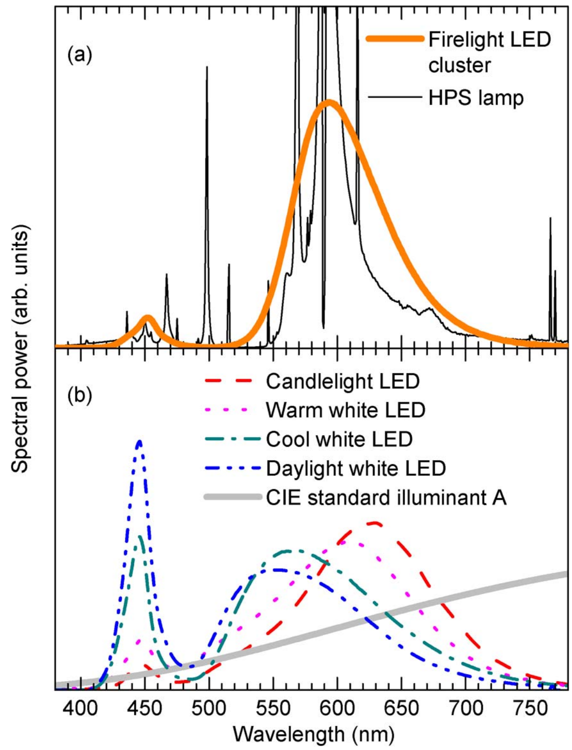

Fig. 1. Spectral power distributions of light sources. (a) Firelight LED cluster (bold line) and HPS lamp (thin line; truncated top). (b) Candlelight (dashed line), warm white (dotted line), cool white (dash-dotted line), and daylight (dash-dot-dotted line) phosphor converted LEDs and CIE standard illuminant A (bold gray line).

component LEDs were selected in such a way that the resulting chromaticity of the cluster was as close as possible to that of the reference HPS lamp (Philips model SON-T PIA PLUS 70W E E27 1SL with an electronic ballast) and the minimal ratio of the circadian action to mesopic luminous efficacy of radiation (MLER) was attained [25]. The LEDs were mounted on a metal-core printed-circuit board within an area of 13×16 mm^2 and the board was attached to a massive heat sink. The ratio of the amber and blue spectral components within the cluster was precisely adjusted using buck LED drivers (Diodes, Inc. model AL8805). The SPD was calibrated using a Labsphere model Illumia Pro Light measurement system consisting of a 50-cm integrating sphere and a spectrometer SMS 500.

3. Assessment of SPDs

Fig. 1(a) displays the SPDs of the firelight LED cluster and HPS lamp with equal integral radiant power. In comparison with the structured SPD of the HPS lamp, the LED cluster is seen to have a smooth SPD with an increased spectral power in the red (around 630 nm) and yellow-green (540–580 nm) ranges of the spectrum and a reduced spectral power at the peaks of the main lines of sodium emission. Also, a characteristic feature of the dichromatic firelight LED cluster is a very low spectral power in the cyan-green (480–520 nm) range due to a Eu^{2+} activated amber phosphor with a moderate width of the band used.

Fig. 1(b) shows the SPDs of other light sources used for the comparative assessment of the firelight LED cluster: quasi-white "candlelight," warm white, cool white, and daylight pc LEDs (Stanley model GTDW1656JTE-20Y and Philips Lumileds models Luxeon Rebel LXM8-PW27, LXML-PWN2, and LXML-PWC2, respectively), and the CIE standard illuminant A. Not shown is the SPD of low-pressure sodium (LPS) lamp (SOX), which contains a narrow duplet of 589.0 nm and 589.6 nm lines. In comparison with the firelight LED cluster, the SPDs of the common pc white

TABLE 1

Photometric and colorimetric properties of the light sources

Light source	CCT (K)	Chromaticity coordinates		S/P	(M)LER (lm/W)		
		x	y		0.1 $\mathrm{cd/m^2}$	2 $\mathrm{cd/m^2}$	photopic
LPS lamp	1814	0.5669	0.4324	0.23	380	493	517
HPS lamp	1886	0.5390	0.4104	0.54	325	376	387
Firelight LED cluster	**1859**	**0.5424**	**0.4101**	**0.49**	**295**	**347**	**358**
Candlelight pc LED	2001	0.5215	0.4067	0.85	249	260	263
Warm white pc LED	2725	0.4582	0.4114	1.19	331	314	311
Cool white pc LED	3991	0.3839	0.3893	1.39	388	350	342
Daylight white pc LED	6084	0.3207	0.3287	1.92	414	332	314
CIE standard illuminant A	2854	0.4475	0.4074	1.41	178	160	156

LEDs, which are optimized for high color rendering, have broader long-wavelength bands due to Ce^{3+} activated phosphors or diphosphor composition of the wavelength converter.

3.1. Photometric, Colorimetric, and Color Rendition Properties of the Light Sources

The most relevant photometric and colorimetric properties of the sources under assessment are presented in Table 1. The ratio of scotopic to photopic weighted lumen outputs (S/P ratio) for an SPD $S(\lambda)$ (λ is the wavelength) is defined as

$$\mathrm{S/P} = K_0' \int_{380\,\mathrm{nm}}^{780\,\mathrm{nm}} V'(\lambda)S(\lambda)\,\mathrm{d}\lambda \Big/ K_0 \int_{380\,\mathrm{nm}}^{780\,\mathrm{nm}} V(\lambda)S(\lambda)\,\mathrm{d}\lambda, \tag{1}$$

where $V(\lambda)$ and $V'(\lambda)$ are the CIE scotopic and photopic spectral luminous efficiency functions, respectively, and $K_0' = 1700$ lm/W and $K_0 = 683$ lm/W are the maximum values of spectral luminous efficacy for scotopic and photopic vision, respectively.

The MLER was estimated by weighting the SPDs by mesopic luminous efficiency function $V_{\mathrm{mes}}(\lambda)$ of the MES-2 visual-performance-based photometric system [28]

$$\mathrm{MLER} = K_{\mathrm{mes0}} \int_{380\,\mathrm{nm}}^{780\,\mathrm{nm}} V_{\mathrm{mes}}(\lambda)S(\lambda)\,\mathrm{d}\lambda \Big/ \int_{380\,\mathrm{nm}}^{780\,\mathrm{nm}} S(\lambda)\,\mathrm{d}\lambda, \tag{2}$$

where $K_{\mathrm{mes0}} = K_0/V_{\mathrm{mes}}$ (555 nm) is the maximum value of spectral luminous efficacy for mesopic vision. Beyond the endpoints of the mesopic range of adaptation luminances (0.005 cd/m^2 and 5 cd/m^2), the mesopic luminous efficacy function and the maximum value of spectral luminous efficacy have the values that correspond to scotopic and photopic vision, respectively.

In Table 1, the values of MLER are presented for two values of mesopic luminance that delimit the upper part of the mesopic region relevant to outdoor lighting, 0.1 cd/m^2 (lowest-class pedestrian area, $\sim$2 lx illuminance) and 2 cd/m^2 (highest class road), respectively. Also, the photopic values of LER are presented.

The S/P ratio and MLER of the firelight LED cluster is seen to be by 10% smaller than that of the HPS lamp. The S/P ratio of the LPS lamp is much smaller, whereas it is considerably larger for common LEDs. Despite this, owing to the optimized SPD the firelight LED cluster has MLER comparable to that of common cool white pc LED at an adaptation luminance of 2 cd/m^2 and exceeds the MLER of the candlelight LED by 18% at an adaptation luminance of 0.1 cd/m^2. However, at the latter low adaptation luminance, blue-enriched SPDs of warm white, cool white, and daylight pc LEDs have higher MLERs than the blue-deficient one of the firelight LED cluster. The CIE 1931 chromaticity coordinates of the firelight LED cluster and HPS lamp are depicted by solid points in Fig. 2. The chromaticity coordinates of the two sources do not deviate from the Planckian

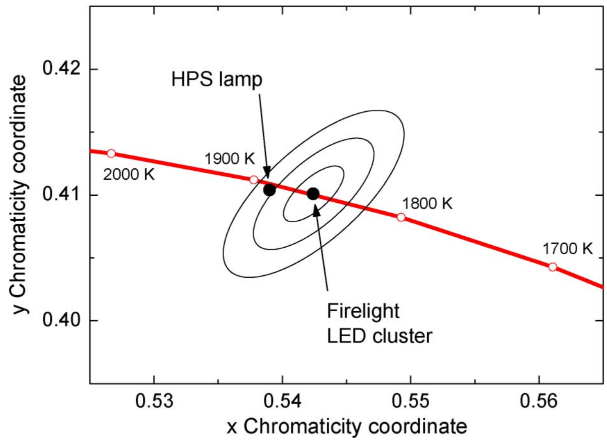

Fig. 2. Solid points, chromaticity coordinates of the firelight LED cluster, and HPS lamp within a segment of the CIE 1931 diagram. The Planckian locus and MacAdam ellipses of 1, 2, and 3 steps centered at the chromaticity coordinates of the LED cluster are shown by bold and fine lines, respectively.

TABLE 2

Color rendition indices of the light sources

Light source	R_a equivalent 0.1 $\mathrm{cd/m^2}$	R_a equivalent 2 $\mathrm{cd/m^2}$	R_a equivalent photopic	GAI	CFI	CSI	CDI	HDI	LDI
LPS lamp	76	25	-47	0.1	3	0	95	0	80
HPS lamp	86	55	12	17	9	0	84	38	69
Firelight LED cluster	**90**	**68**	**37**	**24**	**9**	**1**	**79**	**32**	**63**
Candlelight pc LED	97	92	84	36	51	0	39	5	18
Warm white pc LED	97	91	82	50	43	0	43	11	24
Cool white pc LED	95	83	66	67	18	5	57	48	47
Daylight white pc LED	96	86	72	89	19	5	51	50	45
CIE standard illuminant A	100	100	100	56	100	0	0	0	0

locus (bold line in Fig. 2) by more than $\Delta xy \sim 0.0004$. The HPS lamp has a somewhat higher CCT of 1886 K than the LED cluster (1859 K). However, the two light sources are almost metameric with the chromaticity difference falling within a 3-step MacAdam ellipse (the fine lines in Fig. 2 show MacAdam ellipses of 1, 2, and 3 steps obtained by the geodesic interpolation method [29]).

Table 2 presents the color rendition indices of the light sources under assessment. The values of the CIE general color rendering index (R_a) [30] are presented for standard photopic conditions, as well as for mesopic conditions with the rescaling of the color shifts due to the reduced color discrimination ability of human vision taken into account [25]:

$$R_{a,mes} = 100 - \gamma(L_{mes})(100 - R_a). \tag{3}$$

Here, $\gamma(L_{mes})$ is the color shift rescaling factor, which is the ratio of the mean size of the MacAdam ellipses at photopic conditions to that at a particular mesopic luminance. The values of the rescaling factor deduced from the mean size of MacAdam ellipses at mesopic conditions [31], [32] equal 0.16 and 0.51 for adaptation luminances of 0.1 cd/m^2 and 2 cd/m^2, respectively.

Also, shown in Table 2 are the gamut area index (GAI) [33] and the statistical color rendition indices obtained from the statistical analysis of the color-shift vectors for 1269 Munsell test color samples in respect of 3-step MacAdam ellipses and 2% lightness toleration [29]: the color fidelity index (CFI), color saturation index (CSI), color dulling index (CDI), hue distortion index (HDI), and lightness distortion index (LDI), which are the percentages of colors rendered with high fidelity, increased chroma, decreased chroma, distorted hue, and distorted lightness, respectively.

The LPS lamp is seen to have no color fidelity (negative R_a and very low CFI) and highly shrunk gamut area (low GAI); it renders colors with almost lost chroma (the CDI is such high that hue distortions are not resolved at all) and high distortions of luminance. This makes this light source inappropriate for illumination of most environments, except for very low luminances when the color discrimination ability of human vision is very low.

In the photopic limit, R_a and GAI of the firelight LED cluster is seen to be as 3 times and 1.4 times higher than that of HPS lamp, respectively, although these indices are much smaller than those of common candlelight and white pc LEDs. Meanwhile at mesopic conditions, the rescaled (equivalent) values of R_a show that the latter drawback of the firelight LED cluster is mitigated making this index comparable with that of common pc LEDs at photopic conditions. It is to be noted that for adaptation luminances typical of outdoor lighting, most common white pc LEDs with blue-enriched SPD have the equivalent values of R_a that can be considered as redundant [34].

A deeper insight into the color rendition properties based on the statistical analysis of the color shift vectors for a large number of test color samples shows that the reduced color fidelity (reduced CFI values) of both solid-state and sodium-based sources considered is due mainly to a large number of colors rendered with reduced chroma (increased CDI values). All sources do almost not render colors with increased chroma (low CSI values) and many colors are rendered with distorted hue and chroma (high HDI and LDI values, respectively).

3.2. Circadian Action

The quantification of circadian response to a light source is a complex problem that is not completely resolved for all conditions. So far, the scientific community reached a consensus only on that the circadian action increases with increasing retinal irradiance and shifting the light source spectrum to shorter wavelengths [35]. The simplest model of the spectral sensitivity of the human circadian system introduced by Gall [36] is based on a single spectral circadian efficiency function $C(\lambda)$, which approximates the experimental action spectra of melatonin suppression [7], [8]. Within such an approach, the circadian action of light for adaptation luminances relevant to outdoor lighting can be quantified by a mesopic melatonin suppression index (MMSI), which is defined as the melatonin suppression efficacy of radiation per unit mesopic luminous flux. For ease of scaling, here we normalized the value of MMSI for a light source under assessment to that for the CIE standard illuminant A per unit photopic luminous flux as follows:

$$\mathrm{MMSI_A} = \frac{\int_{380\,\mathrm{nm}}^{780\,\mathrm{nm}} C(\lambda)S(\lambda)\,\mathrm{d}\lambda}{K_{\mathrm{mes}0}\int_{380\,\mathrm{nm}}^{780\,\mathrm{nm}} V_{\mathrm{mes}}(\lambda)S(\lambda)\,\mathrm{d}\lambda} \Bigg/ \frac{\int_{380\,\mathrm{nm}}^{780\,\mathrm{nm}} C(\lambda)S_{\mathrm{A}}(\lambda)\,\mathrm{d}\lambda}{K_0\int_{380\,\mathrm{nm}}^{780\,\mathrm{nm}} V(\lambda)S_{\mathrm{A}}(\lambda)\,\mathrm{d}\lambda} \tag{4}$$

where $S_A(\lambda)$ is the SPD of the CIE standard illuminant A.

The approach of Gall suffers from that it is based on melatonin suppression action spectra measured under narrow-band light. Rea *et al.* [37] introduced a non-linear approach, which accounts for the circadian action due a spectral opponent input to the ipRGC from the blue-yellow visual channel (S-cone excitation). This approach is claimed to be suitable for both wide-band (polychromatic) and narrow-band light, although it lacks independent validation. With a glance to the mesopic sensitivity of the human eye, the photopic circadian light of a light source normalized to that of the CIE standard illuminant A (CL_A [37]) can be converted to a mesopic circadian light index $MCLI_A$ as follows:

$$\mathrm{MCLI_A} = \frac{\mathrm{CL_A}}{1000} \times \frac{\mathrm{LER}}{\mathrm{MLER}} \tag{5}$$

where LER and MLER are the photopic and mesopic LERs of the light source SPD defined by Eq. (2).

TABLE 3

Melatonin suppression indices of the light sources

Light source	CCT (K)	(M)MSI$_A$			(M)CLI$_A$		
		0.1 cd/m^2	2 cd/m^2	photopic	0.1 cd/m^2	2 cd/m^2	photopic
LPS lamp	1814	0.06*	0.05*	0.05*	0.06	0.05	0.05
HPS lamp	1886	0.36	0.31	0.30	0.38	0.33	0.32
Firelight LED cluster	**1859**	**0.28**	**0.24**	**0.23**	**0.29**	**0.25**	**0.24**
Candlelight pc LED	2001	0.50	0.48	0.48	0.55	0.53	0.52
Warm white pc LED	2725	0.76	0.80	0.81	0.78	0.82	0.83
Cool white pc LED	3991	1.03	1.14	1.16	0.41	0.45	0.46
Daylight white pc LED	6084	1.53	1.91	2.02	0.94	1.18	1.24
CIE standard illuminant A	2854	0.87	0.97	1	0.87	0.97	1

*Since the Gall function is not defined for wavelengths longer than 580 nm, the (M)MSI$_A$ values for LPS lamp are equated to the corresponding (M)CLI$_A$ ones.

Further improving the model of circadian spectral sensitivity might require accounting for such conditions as the duration, periodicity, and time of day of exposure to light, as well as for non-linear response in respect of illuminance level and the long-wavelength enhancement of blue-light effect due to melanopsin bistability [38].

Despite some limitations, here we present the results of assessment of solid-state and sodium-based light sources using the above two models described by Eqs. (4) and (5), respectively. The estimated values of the circadian factors are shown in Table 3 for two mesopic luminances and in the photopic limit. Basically, both factors are seen to have very similar values for the sources with low CCTs; they increase with increasing CCT (the spectral opponent effect manifests itself in considerably lower values of MCLI$_A$ in respect of MMSI$_A$ for cool white and daylight LEDs). The LPS lamp, which has a limited applicability in outdoor lighting due to color rendering issues, has the lowest values of the circadian action factors.

Due to the optimized SPD, the firelight LED cluster is seen to have by 22–25% lower values of the circadian factors in comparison with the metameric HPS lamp and about twice as lower values in comparison with the common candlelight pc LED. The effect is even higher when the firelight LED is compared to common warm white and daylight pc LEDs.

3.3. Light Pollution

Nocturnal skyglow due to light reflected upward from illuminated outdoor surfaces is the most difficult to avoid light pollution provided by solid-state light sources. Generally, skyglow occurs due to molecular and aerosol scattering of light in the atmosphere. Molecular and aerosol scattering is described by the Rayleigh and Mie theories, respectively, with the scattering cross-section strongly dependent on the wavelength as λ^{-4} in the former case and with typically less wavelength-sensitive cross-section (scaled with λ^{-1}) in the latter case. Additionally in both cases, the observed luminance of skyglow depends on the distance from the light source [18], [39].

Based on solely Rayleigh scattering, an approach that allows for quantitatively comparing light sources within the hypothetical limit of scatter by only sub-wavelength size particles at short distances can be introduced [17], [40]. Here, we assess the light sources by three different indices that quantify the limiting (Mie scattering free) effect of SPD on skyglow per unit mesopic luminous flux provided by a source. The indices relevant to three different observation conditions under Rayleigh skyglow are as follows: i) the mesopic general visual index (MGVI$_A$) relevant to visually perceived skyglow in the entire visible spectrum; ii) the mesopic filtered visual index (MFVI$_A$) relevant to visual observation trough an optical band-pass optical filter; and iii) the mesopic filtered instrumental index (MFII$_A$) relevant to the detection of photons through the same optical band-pass filter. For the ease of scaling, all the three indices are normalized to the corresponding values for the CIE standard illuminant A per unit photopic luminous flux.

TABLE 4

Mesopic Rayleigh skyglow indices of the light sources

Light source	(M)GVI$_A$			(M)GVI$_A$			(M)GVI$_A$		
	0.1 $\mathrm{cd/m^2}$	2 $\mathrm{cd/m^2}$	phot.	0.1 $\mathrm{cd/m^2}$	2 $\mathrm{cd/m^2}$	phot.	0.1 $\mathrm{cd/m^2}$	2 $\mathrm{cd/m^2}$	phot.
LPS lamp	0.13	0.10	0.09	0.00	0.00	0.00	0.00	0.00	0.00
HPS lamp	0.40	0.35	0.34	0.29	0.25	0.24	0.29	0.25	0.24
Firelight LED cluster	**0.35**	**0.30**	**0.29**	**0.17**	**0.15**	**0.14**	**0.23**	**0.19**	**0.19**
Candlelight pc LED	0.58	0.55	0.55	0.50	0.48	0.48	0.53	0.51	0.51
Warm white pc LED	0.77	0.81	0.82	0.73	0.77	0.78	0.77	0.81	0.82
Cool white pc LED	0.89	0.98	1.01	0.79	0.87	0.90	0.96	1.06	1.09
Daylight white pc LED	1.16	1.44	1.52	1.13	1.41	1.49	1.39	1.73	1.83
CIE standard illuminant A	0.87	0.97	1.00	0.87	0.97	1.00	0.87	0.97	1.00

The MGVI$_\mathrm{A}$ is derived from the SPD of a light source weighted by the scotopic luminous efficacy function and Raleigh scattering factor λ^{-4} in the entire range of visible spectrum as follows:

$$\mathrm{MGVI_A} = \frac{\int_{380\,\mathrm{nm}}^{780\,\mathrm{nm}} \lambda^{-4} V'(\lambda) S(\lambda)\,\mathrm{d}\lambda}{K_{\mathrm{mes0}} \int_{380\,\mathrm{nm}}^{780\,\mathrm{nm}} V_{\mathrm{mes}}(\lambda) S(\lambda)\,\mathrm{d}\lambda} \Bigg/ \frac{\int_{380\,\mathrm{nm}}^{780\,\mathrm{nm}} \lambda^{-4} V'(\lambda) S_\mathrm{A}(\lambda)\,\mathrm{d}\lambda}{K_0 \int_{380\,\mathrm{nm}}^{780\,\mathrm{nm}} V(\lambda) S_\mathrm{A}(\lambda)\,\mathrm{d}\lambda}. \tag{6}$$

The MFVI$_\mathrm{A}$ differs from MGVI$_\mathrm{A}$ in that the weighting is performed within the "protected" band of 440 nm to 540 nm, which can be isolated using an appropriate optical band-pass filter [17]:

$$\mathrm{MFVI_A} = \frac{\int_{440\,\mathrm{nm}}^{540\,\mathrm{nm}} \lambda^{-4} V'(\lambda) S(\lambda)\,\mathrm{d}\lambda}{K_{\mathrm{mes0}} \int_{380\,\mathrm{nm}}^{780\,\mathrm{nm}} V_{\mathrm{mes}}(\lambda) S(\lambda)\,\mathrm{d}\lambda} \Bigg/ \frac{\int_{440\,\mathrm{nm}}^{540\,\mathrm{nm}} \lambda^{-4} V'(\lambda) S_\mathrm{A}(\lambda)\,\mathrm{d}\lambda}{K_0 \int_{380\,\mathrm{nm}}^{780\,\mathrm{nm}} V(\lambda) S_\mathrm{A}(\lambda)\,\mathrm{d}\lambda}. \tag{7}$$

The MFII$_\mathrm{A}$ differs from MFVI$_\mathrm{A}$ in that the spectral power of the glow and the scotopic luminous efficiency function are replaced by the spectral photon flux, which is proportional to $\lambda S(\lambda)$, and a wavelength independent instrumental response function, respectively:

$$\mathrm{MFII_A} = \frac{\int_{440\,\mathrm{nm}}^{540\,\mathrm{nm}} \lambda^{-3} S(\lambda)\,\mathrm{d}\lambda}{K_{\mathrm{mes0}} \int_{380\,\mathrm{nm}}^{780\,\mathrm{nm}} V_{\mathrm{mes}}(\lambda) S(\lambda)\,\mathrm{d}\lambda} \Bigg/ \frac{\int_{440\,\mathrm{nm}}^{540\,\mathrm{nm}} \lambda^{-3} S_\mathrm{A}(\lambda)\,\mathrm{d}\lambda}{K_0 \int_{380\,\mathrm{nm}}^{780\,\mathrm{nm}} V(\lambda) S_\mathrm{A}(\lambda)\,\mathrm{d}\lambda}. \tag{8}$$

Table 4 presents the results of the assessment of the solid-state and sodium-based light sources by the three limiting Raleigh skyglow indices. (Note that when two light sources are compared by the ratio of corresponding limiting indices, the actual ratio of the skyglow luminance is smaller due to Mie scattering.) The general visual index MGVI$_\mathrm{A}$ shows a tendency to increase with increasing CCT; also, with increasing luminance it increases for blue-enriched SPDs and decreases for blue-deficient sources. The lowest values of MGVI$_\mathrm{A}$ are achieved for monochromatic LPS lamp. The firelight LED cluster has about as three times as higher values of MGVI$_\mathrm{A}$ than those of the LPS lamp, but by 12–15% lower values in comparison with the HPS lamp. When compared to common white pc LEDs, the short-distance Rayleigh scattering effect of the firelight LED cluster is smaller by a factor of 1.7 to 5.2 depending on the type of pc LED and adaptation luminance it provides with.

For filtered visual Raleigh skyglow (MFVI$_\mathrm{A}$), the effect of the LPS lamp can be completely eliminated, whereas the firelight LED cluster performs even better than in the general case. The reduction of MFVIA in respect of the HPS lamps is by about 40% and by a factor of 2.9 to 6.4 in respect of the common white pc LEDs. For filtered instrumental Raleigh skyglow (MFII$_\mathrm{A}$), the

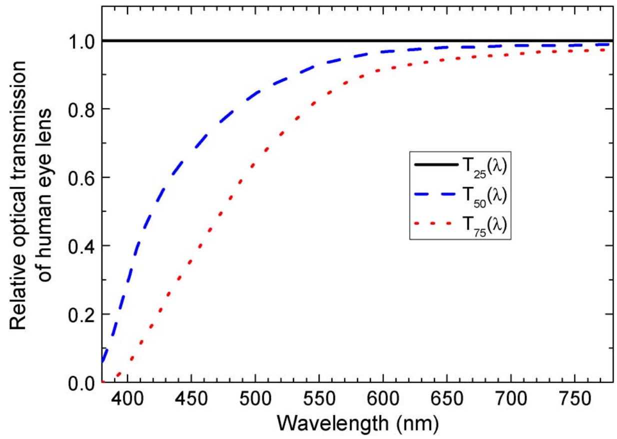

Fig. 3. Normalized transmission spectra of the lens of the human eye at ages of 25 (solid line), 55 (dashed line), and 75 (dotted line) [20], [41].

TABLE 5

Mesopic eye lens yellowing indices of the light sources

Light source	CCT (K)	MLYI_{50}			MLYI_{75}		
		0.1 $\mathrm{cd/m^2}$	2 $\mathrm{cd/m^2}$	photopic	0.1 $\mathrm{cd/m^2}$	2 $\mathrm{cd/m^2}$	photopic
LPS lamp	1814	0.96	0.96	0.96	0.90	0.90	0.90
HPS lamp	1886	0.94	0.95	0.96	0.86	0.89	0.89
Firelight LED cluster	**1859**	**0.94**	**0.95**	**0.96**	**0.87**	**0.89**	**0.89**
Candlelight pc LED	2001	0.93	0.94	0.95	0.83	0.87	0.87
Warm white pc LED	2725	0.91	0.93	0.94	0.80	0.85	0.86
Cool white pc LED	3991	0.90	0.93	0.93	0.77	0.83	0.84
Daylight white pc LED	6084	0.87	0.91	0.93	0.73	0.81	0.83
CIE standard illuminant A	2854	0.90	0.93	0.94	0.78	0.84	0.85

reduction is by about 20% in respect of the HPS lamp and by a factor of 2.3 to 5.7 for the common white pc LEDs, respectively. For filtered skyglow, the impact of the firelight LED cluster can be reduced even more at an expense of observed luminance or detected radiance provided that an optical filter with a narrower band, e.g., 480–520 nm is used.

3.4. Eye Lens Yellowing

For outdoor lighting applications, the effect of reduced retinal illuminance due to the yellowing of the lens of the human eye with age can be quantified by the mesopic lens yellowing index MLYI, which is defined as follows:

$$\mathrm{MLYI}_{\mathrm{age}} = \int_{380\,\mathrm{nm}}^{780\,\mathrm{nm}} V_{\mathrm{mes}}(\lambda) T_{\mathrm{age}}(\lambda) S(\lambda)\,\mathrm{d}\lambda \Big/ \int_{380\,\mathrm{nm}}^{780\,\mathrm{nm}} V_{\mathrm{mes}}(\lambda) T_{25}(\lambda) S(\lambda)\,\mathrm{d}\lambda \quad (9)$$

where $T_{\mathrm{age}}(\lambda)$ and $T_{25}(\lambda)$ are the transmission spectra of the lens of the human eye at a particular age and at an age of 25, respectively. Fig. 3 shows the transmission spectra of the lens at ages of 50 and 75 normalized to that at an age of 25 [20], [41].

Table 5 presents the results of the assessment of light sources by MLYI for ages 50 and 75. Basically for all sources, some reduction in retinal illuminance is found with reducing the ambient luminance due to the shift of the luminous efficiency function to shorter wavelengths. This effect is seen to be higher for blue-enriched SPDs. The firelight LED cluster performs very similarly to sodium based sources showing a reduction of transmittivity due to the yellowing by factors of 0.94 and 0.87 at the lowest mesopic luminance of 0.1 cd/m^2 for ages of 50 and 75, respectively. For common pc white LEDs, the MLYI has smaller values depending on the CCT and age. For instance at a luminance of 0.1 cd/m^2, the MLYI of the firelight LED cluster is higher by 8% and 19% in respect of the daylight pc LED for ages of 50 and 75, respectively. Although these differences might appear small, they might be comparable to the differences between luminances specified for adjacent road lighting classes (from 33% to 67%).

4. Psychophysical Assessment

The psychophysical assessment of the firelight LED cluster was carried out by comparing it to the almost metameric HPS lamp, which is a well-established light source for outdoor lighting, within the visual performance based approach under mesopic visual conditions [42], [43]. Three visual performance tasks that are the most relevant to night-time driving and pedestrian walking and are commonly applied for the comparative studies of different outdoor light sources were selected as follows: detection response to a visual stimulus [44]–[47], contrast discrimination [45], [47]–[49], and color discrimination [41], [50], [51]. In this paper, the three tasks were executed by the measurements of reaction time and correct detection rate, the detection threshold of achromatic contrast, and the error rate in the Farnsworth-Munsell (F-M) 100-hue test, respectively.

The experiments were performed for four photopic adaptation luminance values of 0.1, 0.3, 1.0, and 3.0 cd/m^2 covering the upper part of the mesopic region, which is important for night-time driving and pedestrian walking. The corresponding mesopic luminances within the MES-2 photometric system [28] equaled 0.084, 0.275, 0.953, and 2.948 cd/m^2 for the HPS lamp and 0.081, 0.272, 0.947, and 2.942 cd/m^2 for the firelight LED cluster, respectively, i.e., differed by less than 4% and by 0.2% at the lowest and highest luminance used, respectively.

The two sources of light were mounted on top of two respective experimental cabinets (80 cm height by 70 cm width by 70 cm depth) with neutral gray matted interior and ceiling made of Plexiglas. The ceiling was used for uniformly distributing luminance over the walls of the cabinets (with an unevenness of less than 5% at the bottom surface of a cabinet) and for color mixing (the chromaticity point was maintained within a distance of $\Delta xy \sim 0.005$ across the bottom surface of a cabinet). The luminance was controlled by a diaphragm and an additional frosted glass filter placed between a lamp and the ceiling and monitored by an imaging photometer-colorimeter (Instruments Systems model LumiCam 1300 Color).

A homogeneous group of four thoroughly instructed and well trained young subjects took part in the experiment. Of those one was female and three were males; the age ranged from 22 to 25 in order to avoid the effects related to the yellowing of the human eye lens. All subjects had normal or corrected to normal visual acuity and normal color vision tested by the F-M 100-hue test under photopic conditions. Subjects sat next to the cabinet placed in a dark room with the head fully immersed into the cabinet in order to ensure 180 deg. adaptation to the visual field. For each subject, experiments were performed with the luminance level gradually incremented form the lowest one to the highest one within multiple sessions that were scheduled at different days. In each session, the lamps were presented in a random sequence. Before starting the measurements, observers adapted to the illuminance level of the background for a minimum of 10 min at a luminance of 0.1 cd/m^2 and then for a minimum of 5 min for each higher luminance level, which are typical times of adaptation to mesopic luminance conditions [52].

The results of the experiments on the three tasks were aggregated for all subjects and execution sessions and the mean values and 95% confidence intervals were calculated for each luminance/source condition as presented by data points and error bars in the figures below. The significance of the differences between each pair of data points for the two sources were analyzed using a *t*-test.

4.1. Reaction Time

For the measurement of reaction time, a rotating stimulus [3] placed with 18°. right peripheral eccentricity within a cabinet was used. In order to maintain the eccentricity, the head of observer

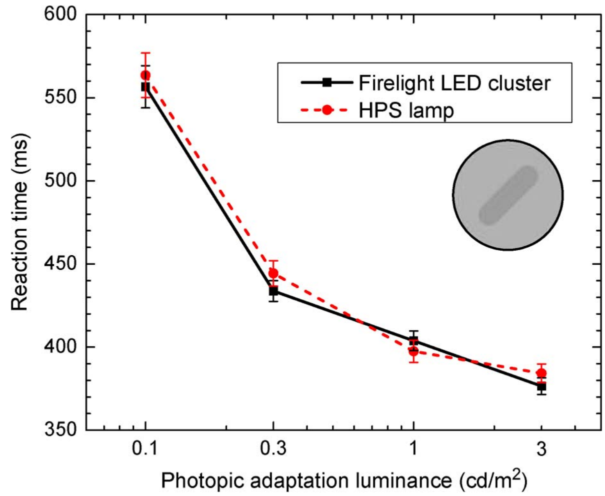

Fig. 4. Time of reaction to the achromatic off-axis rotating stimulus as a function of photopic adaptation luminance for the firelight LED cluster (rectangles) and HPS lamp (circles). The error bars show the 95% confidence intervals. The lines are a guide for the eye. The insert displays an image of the rotating stimulus.

was mildly restrained within a chinrest and the view was positioned at a fixation point centered on the back wall of the cabinet at a distance of 60 cm. The stimulus comprised an achromatic circular patch with a luminance similar to that of the cabinet interior and with a centered darker rectangular bar (2 by 0.5 deg. of visual angle, which is relevant to driving tasks; see insert in Fig. 4. The Weber contrast $(L_b - L_p)/L_p$ of the bar to patch background, as calculated basing on the measurement results provided by the imaging photometer-colorimeter, equaled -0.3 (L_b and L_p are the bar and patch background luminances, respectively). The patch was mounted on a computer controlled stepper motor that moved clockwise or anticlockwise into two random positions tilted by 45 deg. in respect of the vertical (characterized as "right" and "left, " respectively) within random intervals of 5 to 15 s. Once subject noticed the motion (120 ms long) he/she ought to execute a simple decision-making task by pressing a respective button of a computer mouse and the reaction time in respect of the termination of the motion was recorded. A detection error was recorded if no correct response was received in 1500 ms on the first attempt. Each of four subjects executed seven sessions with 40 repeated measurements for each luminance level provided by each source.

Fig. 4 displays the dependence of reaction time on photopic luminance for the achromatic off-axis stimulus under lighting conditions provided by the firelight LED cluster (rectangles) and HPS lamp (circles). Each point presents a mean of 280 attempts for each of four subjects (1120 attempts in total). The reaction time increases from about 380 ms to about 560 ms with decreasing adaptation luminance from 3 to 0.1 cd/m^2. The results for the two sources show no statistically significant differences at luminances of 0.1 and 1 cd/m^2 ($p > 0.15$) and small differences with a moderate significance at luminances of 0.3 and 3 cd/m^2 ($p = 0.036$ and $p = 0.044$, respectively) can be resolved. These measured values of reaction time are larger and exhibit a stronger dependence on luminance than those measured for a HPS lamp for an off-axis stimulus without decision-making ($\sim$240–270 ms [44]) and smaller than those measured using a driving simulator ($\sim$650–800 ms [47]).

Fig. 5 shows the corresponding dependence of the correct detection rate as a function of photopic adaptation luminance for the firelight LED cluster (rectangles) and HPS lamp (circles). Each point presents a mean of 28 sessions. These data are in line with similar measurements for an HPS lamp [47]. At adaptation luminances of 0.3–3 cd/m^2, the correct detection rate has values around 93% with no statistically significant difference ($p > 0.06$) between the two light sources. At a luminance of 0.1 cd/m^2, a drop of the correct detection rate is observed for both sources with a

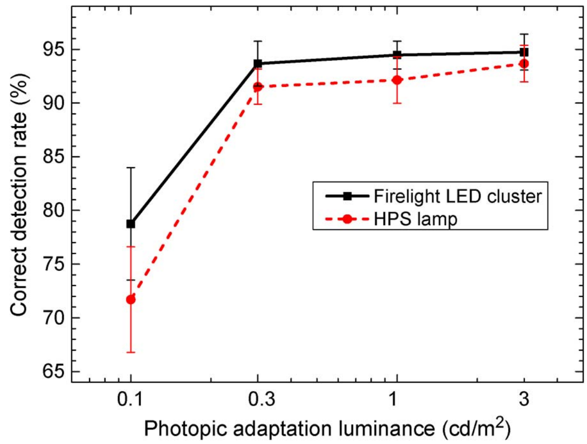

Fig. 5. Rate of the correct detection of the achromatic off-axis rotating stimulus as a function of photopic adaptation luminance for the firelight LED cluster (rectangles) and HPS lamp (circles). The error bars show the 95% confidence intervals. The lines are a guide for the eye.

score of 79% vs. 72% in favor of the firelight LED cluster, but the difference has a low statistical significance ($p = 0.049$).

Our results show that the two sources are almost identical in terms of response to the off-axis achromatic stimulus despite a difference of SPDs (less structured spectrum of the LED cluster as compared to the HPS lamp). This can be attributed to that the S/P ratio and CCT of the two sources are almost equal and provide with both similar involvement of the peripheral retinal receptors into generating a detection response to a visual stimulus and with similar color appearance of achromatic background and target.

4.2. Detection Thresholds of Luminance Contrast

The measurement of the detection thresholds of luminance contrast was performed in the same cabinets. The thresholds were estimated using four sets of 45 circular patches similar to that used in the reaction time measurement (see the insert in Fig. 4), each containing a bar (2 by 0.5 deg. of visual angle) with different Weber luminance contrasts. The patches were arranged into 5×9 tables with sequential increase of Weber contrast from about -0.3 to $+0.3$ with comparable increments of 0.014 on the average. The bars were tilted by ± 45 deg. in a random sequence and each of four tables differed in the randomization of the tilting. The tables were printed on A5 format matted photo paper with 256 bit contrast resolution. The tables were placed on the bottom surface of the cabinets. After adaptation, subjects had to choose two patches with the lowest detected opposite (positive and negative) luminance contrast and tell the orientation and number indicated below them. The detection threshold was estimated as an average of the moduli of the two contrasts. Each subject executed five sessions with each of four tables for each specific luminance/source condition without limiting the execution time. During a session, the tables were presented in a random sequence.

The two light sources were found to have very similar properties in terms of achromatic contrast discrimination. Fig. 6 shows the detection threshold of luminance contrast as a function of photopic adaptation luminance for our targets. Each point presents a mean of 20 attempts for each of four subjects (80 attempts in total). The threshold contrast is seen to increase from about 0.025 to about 0.05 when the background luminance decreases from 3 to 0.1 cd/m^2 with no statistically significant difference between the values obtained for the two sources ($p \geq 0.07$). This variation is in line with the well-known results on contrast discrimination [53], [54], although it has a much larger span than that obtained for a HPS lamp using large (10 by 13 deg.) grating targets [45]. Our data imply that contrast discrimination does not depend on SPD at least for metameric sources with almost equal S/P ratio.

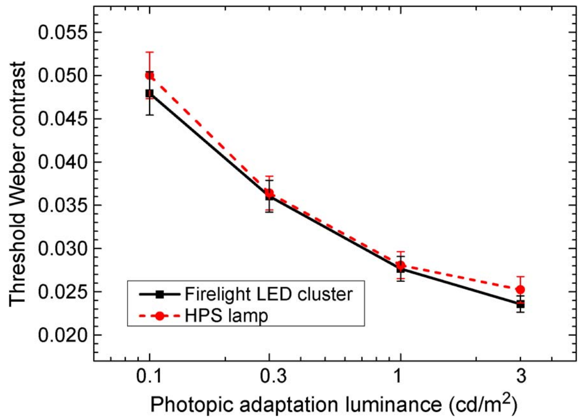

Fig. 6. Detection threshold of luminance contrast as a function of photopic adaptation luminance for the firelight LED cluster (rectangles) and HPS lamp (circles). The error bars show the 95% confidence intervals. The lines are a guide for the eye.

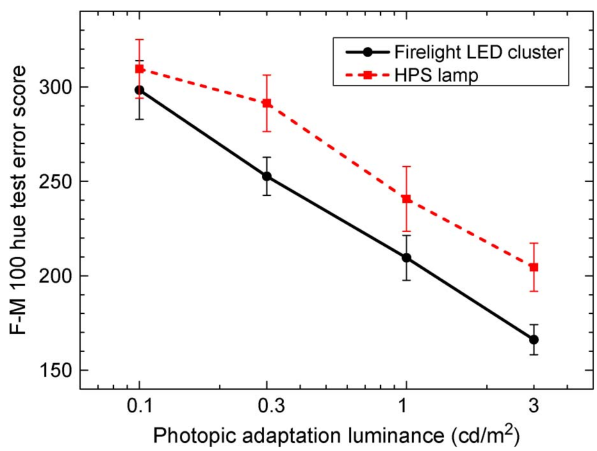

Fig. 7. Farnsworth-Munsell 100-hue test error score as a function of photopic adaptation luminance for the firelight LED cluster (rectangles) and HPS lamp (circles). The error bars show the 95% confidence intervals. The lines are a guide for the eye.

4.3. Fransworth-Munsell 100-Hue Test

The F-M 100-hue test [55] was carried out within the above described cabinets. The test consists of 85 colored caps, which are numbered in sequence and have colors that differ in small increments. The task of a subject is to arrange the caps in the correct hue sequence within four boxes that have two anchor caps at each end. The output of the test is the error score, which is a sum of the absolute differences between the numbers of the arranged caps and the numbers of the adjacent caps with 2 points deduced for each cap. Each subject repeated the test 6 times in different sessions for all specific luminance/source conditions. The execution time was not limited.

Differently from detection response and contrast discrimination, the firelight LED cluster exhibited a noticeable improvement in color discrimination against the HPS lamp. Fig. 7 shows the F-M 100-hue test error score as a function of photopic adaptation luminance for the two light sources. Each point presents a mean of 6 trials for each of four subjects (24 trials in total). The results for the HPS lamp and firelight LED cluster show a gradual increase of the error score from about 205 to 310 and from about 165 to 300, respectively, when the adaptation luminance is reduced from 3 to 0.1 cd/m^2. At an adaptation luminance of 3 cd/m^2, the estimated error scores for both sources are much higher than those for typical fluorescent lamps (30–70) [33]. At a luminance of 0.1 cd/m^2, they exceed those obtained under high-quality daylight illuminant ($\sim$100 [56]) by a factor of about 3. However with exception of the lowest luminance of 0.1 cd/m^2, where the two sources show no significant difference ($p = 0.3$), the error score for the firelight LED cluster is lower than that for the HPS lamp in the rest part of the adaptation luminance range 0.3–3 cd/m^2) with a high statistical significance of the difference ($p < 0.003$).

It is to be noted that the reduction of color discrimination of human vision in the mesopic region does not allow for comparing the error scores of the F-M 100-hue test estimated at different mesopic luminances on the absolute scale. (In fact, such comparing requires a refinement of the F–M 100-hue test by rarefying the set of colored caps for particular luminances in such a way that the hue increments were matched with the altered color discrimination ability.) Despite this limitation, the increase of the F-M 100-test error score with reducing adaptation luminance can be understood in terms of the reduction of color discrimination of human vision in the mesopic region [31]. At the same time the improved color discrimination properties of the firelight LED cluster in respect of the HPS lamp can be attributed to the reduced color shifts and less shrunk gamut represented by higher R_a and GAI values, respectively, as well as by somewhat smaller percentages of colors rendered with reduced chroma and distorted hue and lightness (see Table 2).

5. Conclusion

We have demonstrated a balanced approach to the performance of solid-state lighting for outdoor environments by introducing a practical blue-amber LED cluster, which is a solid-state metamer of HPS lamp. In comparison with a reference HPS lamp, our firelight LED cluster has somewhat smaller mesopic LER, which can be increased to about 400 lm/W by selecting an amber phosphor with a narrower band [25], however. Potentially (under conditions of 100% radiant efficiency of the semiconductor blue emitter) similar firelight LEDs with partial conversion of blue radiation in phosphors can have radiant efficiency of about 75% [26], [57], which converts to mesopic luminous efficacy of about 300 lm/W at a LER of 400 lm/W. Such a luminous efficacy is within the range of limiting efficacies of common white LEDs and is more than twice as higher as that of HPS lamp and 1.5 times higher than that of LPS lamp.

The psychophysical performance of the firelight LED cluster is identical to that of metameric HPS lamp in terms of reaction time and contrast discrimination threshold for achromatic targets. However, the firelight cluster performs noticeably better than HPS lamp in terms of color discrimination as revealed by the F-M 100-hue test. Also, the cluster outperforms HPS lamp in all aspects of color rendition.

Owing to optimized SPD, the firelight LED cluster has lower indices of melatonin suppression and skyglow than those of common white LEDs and even of HPS lamp. In comparison with common white LEDs, the firelight source also provides with some mitigation of the effect of reduced street luminance for elderly drivers caused by the yellowing of the human eye lens with age. It is to be noted that these advantages of the firelight LED cluster are achieved due to a more structured SPD, which is a dichromatic blend with the long-wavelength band of a moderate width. Under photopic conditions, such an SPD results in noticeably lower color fidelity and may severely affect the execution of visual tasks related to color recognition in comparison to common white LEDs. However, under mesopic conditions typical of outdoor lighting, this drawback of the firelight LED cluster is considerably mitigated by the reduced color discrimination ability of the human vision. Moreover, owing to the flexibility of solid-state lighting technology in tailoring SPD, LED sources intermediate between the introduced firelight (1800–1900 K) and common warm white ($\sim$2700–3200 K) ones can be implemented with a tradeoff between unwanted effects of blue-enriched light, on one hand, and color rendering and discrimination, on the other hand.

References

[1] P. R. Boyce, S. Fotios, and M. Richards, "Road lighting and energy saving," *Lighting Res. Technol.*, vol. 41, no. 3, pp. 245–260, Sep. 2009.
[2] F. Li, D. Chen, X. Song, and Y. Chen, "LEDs: A promising energy-saving light source for road lighting," in *Proc. Asia Pac. Power Energy Eng. Conf.*, Wuhan, China, Mar. 27–31, 2009, pp. 2798–2800.

[3] P. Vitta *et al.,* "Energy-saving approaches to solid state street lighting," in *Proc. SPIE*, Sep. 2011, vol. 8123, pp. 81231H-1–81231H-7.

[4] M. S. Shur and A. Žukauskas, "Solid-state lighting: Toward superior illumination," *Proc. IEEE*, vol. 93, no. 10, pp. 1691–1703, Oct. 2005.

[5] E. F. Schubert and J. K. Kim, "Solid-state light sources getting smart," *Science*, vol. 308, no. 5726, pp. 1274–1278, May 2005.

[6] Int. Dark-Sky Assoc. "Visibility, environmental, and astronomical issues associated with blue-rich white outdoor lighting," IDA, Washington, DC, USA, 2010.

[7] G. C. Brainard *et al.,* "Action spectrum for melatonin regulation in humans: Evidence for a novel circadian photoreceptor," *J. Neurosci.*, vol. 21, no. 16, pp. 6405–6412, Aug. 2001.

[8] K. Thapan, J. Arendt, and D. J. Skene, "An action spectrum for melatonin suppression: Evidence for a novel non-rod, non-cone photoreceptor system in humans," *J. Physiol.*, vol. 535, no. 1, pp. 261–267, Aug. 2001.

[9] D. M. Berson, F. A. Dunn, and M. Takao, "Phototransduction by retinal ganglion cells that set the circadian clock," *Science*, vol. 295, no. 5557, pp. 1070–1073, Feb. 2002.

[10] J. M. Zeitzer, D.-J. Dijk, R. E. Kronauer, E. N. Brown, and C. A. Czeisler, "Sensitivity of the human circadian pacemaker to nocturnal light: Melatonin phase resetting and suppression," *J. Physiol.*, vol. 526, no. 3, pp. 695–702, Aug. 2000.

[11] K. P. Wright, R. J. Hughes, R. E. Kronauer, D.-J. Dijk, and C. A. Czeisler, "Intrinsic near-24-h pacemaker period determines limits of circadian entrainment to a weak synchronizer in humans," *Proc. Nat. Acad. Sci. USA*, vol. 98, no. 24, pp. 14027–14032, Nov. 2001.

[12] S. W. Lockley, G. C. Brainard, and C. A. Czeisler, "High sensitivity of the human circadian melatonin rhythm to resetting by short wavelength light," *J. Clin. Endocr. Metab.*, vol. 88, no. 9, pp. 4502–4505, Sep. 2003.

[13] S. M. Pauley, "Lighting for the human circadian clock: Recent research indicates that lighting has become a public health issue," *Med. Hypotheses*, vol. 63, no. 4, pp. 588–596, Apr. 2004.

[14] G. Glickman, R. Levin, and G. C. Brainard, "Ocular input for human melatonin regulation: Relevance to breast cancer," *Neuroendocrinol. Lett.*, vol. 23, no. S2, pp. 17–22, Jul. 2002.

[15] K. E. West *et al.,* "Blue light from light-emitting diodes elicits a dose-dependent suppression of melatonin in humans," *J. Appl. Physiol.*, vol. 110, no. 3, pp. 619–626, Mar. 2011.

[16] L. Bellia, F. Bisegna, and G. Spada, "Lighting in indoor environments: Visual and non-visual effects of light sources with different spectral power distributions," *Build. Environ.*, vol. 46, no. 10, pp. 1984–1992, Oct. 2011.

[17] F. Falchi, P. Cinzano, C. D. Elvidge, D. M. Keith, and A. Haim, "Limiting the impact of light pollution on human health, environment and stellar visibility," *J. Environ. Manage.*, vol. 92, no. 10, pp. 2714–2722, Oct. 2011.

[18] C. B. Luginbuhl, P. A. Boley, and D. R. Davis, "The impact of light source spectral power distribution on sky glow," *J. Quant. Spectrosc. Radiat. Transf.*, vol. 139, pp. 21–26, May 2014.

[19] K. J. Gaston, T. W. Davies, J. Bennie, and J. Hopkins, "Reducing the ecological consequences of night-time light pollution: Options and developments," *J. Appl. Ecol.*, vol. 49, no. 6, pp. 1256–1266, Dec. 2012.

[20] D. Lang, "Energy efficient lighting for the biological clock," in *Proc. SPIE*, Feb. 2011, vol. 7954, pp. 795402-1–795402-12.

[21] A. A. Kruithof, "Tubular luminescence lamps for general illumination," *Philips Tech. Rev.*, vol. 6, no. 3, pp. 65–73, Mar. 1941.

[22] P. R. Boyce and C. Cuttle, "Effect of correlated colour temperature on the perception of interiors and colour discrimination performance," *Lighting Res. Technol.*, vol. 22, no. 1, pp. 19–36, Mar. 1990.

[23] R. G. Davis and D. N. Ginthner, "Correlated color temperature, illuminance level, and the Kruithof curve," *J. Illum. Eng. Soc.*, vol. 19, no. 1, pp. 27–38, Jan. 1990.

[24] F. Viénot, M.-L. Durand, and E. Mahler, "Kruithof's rule revisited using LED illumination," *J. Mod. Opt.*, vol. 56, no. 13, pp. 1433–1446, Jul. 2009.

[25] A. Žukauskas, R. Vaicekauskas, and P. Vitta, "Optimization of solid-state lamps for photobiologically friendly mesopic lighting," *Appl. Opt.*, vol. 51, no. 35, pp. 8423–8432, Dec. 2012.

[26] A. Zabiliūtė, R. Vaicekauskas, P. Vitta, and A. ukauskas, "Phosphor converted LEDs with low circadian action for outdoor lighting," *Opt. Lett.*, vol. 39, no. 3, pp. 563–566, Feb. 2014.

[27] J.-P. Lavallé and M. Aubé, "Optimized optical filter for LED lighting," in *Proc. Conf. Light Poll., Theory, Model., Meas.*, Smolenice, Slovakia, Apr. 15–18, 2013, pp. 87–97.

[28] Commission Internationale de l'Éclairage, Recommended system for mesopic photometry based on visual performance, Vienna, Austria, Central Bur. CIE, CIE Pub. No. 191, 2010.

[29] A. Žukauskas *et al.,* "Statistical approach to color quality of solid-state lamps," *IEEE J. Sel. Topics Quantum Electron.*, vol. 15, no. 6, pp. 1753–1762, Nov./Dec. 2009.

[30] Commission Internationale de l'Éclairage, Method of measuring and specifying colour rendering properties of light sources, Vienna, Austria, Central Bur. CIE, CIE Pub. No. 13.3, 1995.

[31] W. R. J. Brown, "The influence of luminance level on visual sensitivity to color differences," *J. Opt. Soc. Amer.*, vol. 41, no. 10, pp. 684–688, Oct. 1951.

[32] R. W. Pridmore and M. Melgosa, "Effect of luminance of samples on color discrimination ellipses: Analysis and prediction of data," *Color Res. Appl.*, vol. 30, no. 3, pp. 186–197, Jun. 2005.

[33] M. S. Rea and J. P. Freyssinier-Nova, "Color rendering: A tale of two metrics," *Color Res. Appl.*, vol. 33, no. 3, pp. 192–202, Jun. 2008.

[34] A. Žukauskas and R. Vaicekauskas, "Colour rendering of solid-state sources of light under mesopic conditions," in *Proc. AIC Colour, 12th Congr. Int. Colour Assoc.*, Newcastle upon Tyne, U.K., Jul. 8–12, 2013, pp. 1737–1740.

[35] R. J. Lucas *et al.,* "Measuring and using light in the melanopsin age," *Trends Neurosci.*, vol. 37, no. 1, pp. 1–9, Jan. 2014.

[36] D. Gall, "Circadiane lichtgren und deren messtechnische ermittlung," *Licht*, vol. 54, no. 11/12, pp. 1292–1297, Nov./Dec. 2002.

[37] M. S. Rea, M. G. Figueiro, A. Bierman, and R. Hamner, "Modelling the spectral sensitivity of the human circadian system," *Lighting Res. Technol.*, vol. 44, no. 4, pp. 386–396, Dec. 2012.

[38] M. D. Rollag, "Does melanopsin bistability have physiological consequences?" *J. Biol. Rhythm.*, vol. 23, no. 5, pp. 396–399, Oct. 2008.

[39] M. Aubé, J. Roby, and M. Kocifaj, "Evaluating potential spectral impacts of various artificial lights on melatonin suppression, photosynthesis, and star visibility," *PLOS One*, vol. 8, no. 7, pp. e67798-1–e67798-15, Jul. 2013.

[40] A. Bierman, "Will switching to LED outdoor lighting increase sky glow?" *Lighting Res. Technol.*, vol. 44, no. 4, pp. 449–458, Dec. 2012.

[41] P. L. Turner and M. A. Mainster, "Circadian photoreception: Ageing and the eye's important role in systemic health," *Brit. J. Ophthalmol.*, vol. 92, no. 11, pp. 1439–1444, Nov. 2008.

[42] M. Eloholma *et al.,* "Mesopic models—From brightness matching to visual performance in night-time driving: A review," *Lighting Res. Technol.*, vol. 37, no. 2, pp. 155–173, Jun. 2005.

[43] S. Fotios, C. Cheal, and P. Boyce, "Light source spectrum, brightness perception and visual performance in pedestrian environments: A review," *Lighting Res. Technol.*, vol. 37, no. 4, pp. 271–291, Dec. 2005.

[44] Y. He, M. Rea, A. Bierman, and J. Bullough, "Evaluating light source efficacy under mesopic conditions using reaction times," *J. Illum. Eng. Soc.*, vol. 26, no. 1, pp. 125–138, Jan. 1997.

[45] A. L. Lewis, "Visual performance as a function of spectral power distribution of light sources at luminances used for general outdoor lighting," *J. Illum. Eng. Soc.*, vol. 28, no. 1, pp. 37–42, Jan. 1999.

[46] J. D. Bullough and M. S. Rea, "Simulated driving performance and peripheral detection at mesopic and low photopic light levels," *Lighting Res. Technol.*, vol. 32, no. 4, pp. 194–198, Dec. 2000.

[47] R. Lingard and M. Rea, "Off-axis detection at mesopic light levels in a driving context," *J. Illum. Eng. Soc.*, vol. 31, no. 1, pp. 33–39, Jan. 2002.

[48] P. R. Boyce and L. D. Bruno, "An evaluation of high pressure sodium and metal halide light sources for parking lot lighting," *J. Illum. Eng. Soc.*, vol. 28, no. 2, pp. 16–32, Jul. 1999.

[49] S. A. Fotios and C. Cheal, "Predicting lamp spectrum effects at mesopic levels. Part 2: Preferred appearance and visual acuity," *Lighting Res. Technol.*, vol. 43, no. 2, pp. 159–172, Jun. 2011.

[50] P. R. Boyce, "Illuminance, lamp type and performance on a colour discrimination task," *Lighting Res. Technol.*, vol. 8, no. 4, pp. 195–199, Dec. 1976.

[51] M. P. Royer, K. W. Houser, and A. M. Wilkerson, "Color discrimination capability under highly structured spectra," *Color Res. Appl.*, vol. 37, no. 6, pp. 441–449, Dec. 2012.

[52] S. Plainis, I. J. Murray, and W. N. Charman, "The role of retinal adaptation in night driving," *Optometr. Vis. Sci.*, vol. 82, no. 8, pp. 682–688, Aug. 2005.

[53] H. R. Blackwell, "Contrast thresholds of the human eye," *J. Opt. Soc. Amer.*, vol. 36, no. 11, pp. 624–632, Nov. 1946.

[54] W. Adrian, "Visibility of targets: Model for calculation," *Lighting Res. Technol.*, vol. 21, no. 4, pp. 181–188, Dec. 1989.

[55] D. Farnsworth, "The Farnsworth-Munsell 100-hue and dichotomous tests for color vision," *J. Opt. Soc. Amer.*, vol. 33, no. 10, pp. 568–578, Oct. 1943.

[56] K. J. Bowman and B. L. Cole, "A recommendation for illumination of the Farnsworth-Munsell 100-hue test," *Amer. J. Optom. Physiol. Opt.*, vol. 57, no. 11, pp. 839–843, Nov. 1980.

[57] H. F. Ivey, "Color and efficiency of luminescent light sources," *J. Opt. Soc. Amer.*, vol. 53, no. 10, pp. 1185–1198, Oct. 1963.